Lembaran Publikasi Minyak dan Gas Bumi, Vol. 60 No. 1, April 2026 : 51 - 69

BALAI BESAR PENGUJIAN MINYAK DAN GAS BUMI
LEMIGAS

Journal Homepage: http://journal.lemigas.esdm.go.id
ISSN: 2089-3396 e-ISSN: 2598-0300

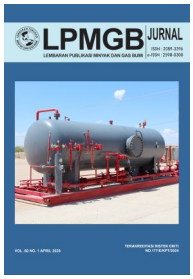

Failure Analysis of Ladle Leakage and Wall Deposit Formation with Low-Nickel Slag Converterin Rotary Kiln–Electric Furnace Nickel Smelting (RKEF)

Fajar Aditya[1], Sutarsis[1], and Meyliana Wulandari[2]

[1]Department of Material and Metallurgical Engineering, Institut Teknologi Sepuluh Nopember, Sukolilo Campus
Teknik Kimia Street, Keputih, Sukolilo District, Surabaya, East Java, 60111, Indonesia.

[2]Department of Chemistry, Faculty of Mathematics and Natural Science, Universitas Negeri Jakarta
Rawamangun Muka Street, Rawamangun, Pulo Gadung, East Jakarta, Jakarta Special Capital Region, 13220, Indonesia.

Article Info:

Manuscript received
February 11th, 2026

Revised
March 25th, 2026

Approved
April 29th, 2026

Published
April 29th, 2026

Keywords:

nickel matte,
ladle failure analysis,
high-nickel slag,
pitting corrosion,
deposit formation.

ABSTRACT

Rotary Kiln Electric Furnace (RKEF) uses ladles to transfer high- and low-nickel slag from the converter at approximately 1200 °C. In 2023, a ladle leak occurred during high-nickel slag handling, cause serious safety and operational risks. This incident necessitated a failure analysis to evaluate ladle material suitability, degradation mechanisms, and the role of slag deposits in ladle integrity. Failure analysis was conducted with Optical Emission Spectroscopy, microstructure test, X-ray Fluorescence, X-ray Diffraction, Scanning Electron Microscopy–Energy Dispersive X-ray, thickness measurement using Non-Destructive Testing, thermal camera, and deposit volume evaluation. Both old (pre-2020) and new (post-2020) ladles were examined. From the test, both ladle types met with ASTM A27 Grade 30–60 specifications. But old ladle categorizes as medium carbon steel (pearlite phase identified) while new ladle categorizes as low carbon steel (ferrite phase identified). Ladle failure was primarily caused by localized mechanical load at the hook ladle during initial high-nickel slag pouring, combined with the absence of a protective low-nickel slag deposit layer, allowing high-nickel slag penetration at elevated temperatures (initial ladle thickness 90 mm, after incident became 39 mm). SEM-EDX identified slag-related compounds, nickel oxide (NiO), which reacted with iron (Fe) to form iron (II) oxide (FeO), inducing pitting corrosion and failure initiation. Adequate deposit volume

during low-nickel slag service provided thermal and chemical protection. Ladles operated at a safe temperature (~335 °C) with a reduced risk of leakage during high-nickel slag and matte handling after the fifth low-nickel slag cycle.

Corresponding author:
E-mail: (faditya68@gmail.com) Fajar Aditya

INTRODUCTION

Downstreaming is a key government initiative aimed at promoting economic growth in the natural resources sector (Of et al., 2024). Nickel is one of the priority minerals due to its extensive distribution in Sulawesi and Maluku. Indonesia possesses the world's largest nickel reserves, approximately 6% of global nickel resources (Pambudi 2025), which are mainly processed through pyrometallurgical process (such as nickel pig iron, ferronickel, and nickel matte) (Iman & Huda 2019).

Several industry that located in Sulawesi, processes laterite nickel into nickel matte via pyrometallurgical routes using Rotary Kiln Electric Furnace (RKEF) technology (Laterite 2019). Nickel matte offers higher nickel purity than other nickel products, reaching approximately 78% (Series & Science 2018). This level of purity is achieved through the incorporation of a converter process, which reduces iron content and consequently increases the nickel concentration in the final product. The converter operates at approximately 1200 °C, producing nickel matte as the primary product and slag as a by product, consisting of low-nickel and high-nickel slag (Industry et al., 2023). Both matte and slag are transported using carbon steel containers known as ladles (Malina 2013). To support continuous production, the company procures these ladles in multiple batches, resulting in the concurrent use of older ladles (manufactured before 2020) and newer ladles (manufactured after 2020).

Ladle in nickel smelting has an issue regarding with the integrity (crack until leakage) because of material formed. Major reason is related with the temperature that absorbed by ladle. Carbon steel as material of ladle only has a safe operational temperature up to 500 °C (Ratna, 2009). If the ladle filled with material that has a temperature above 500 °C, ladle must have an extra treatment to maintain the ladle temperature (usually like deposit or cooling system). High temperature in ladle increases the probability to failure due to corrosion, especially high temperature corrosion like hydrogen embrittlement, stress corrosion cracking that cause pitting. Figure 1 illustrates one of the corrosion mechanisms in carbon steel.

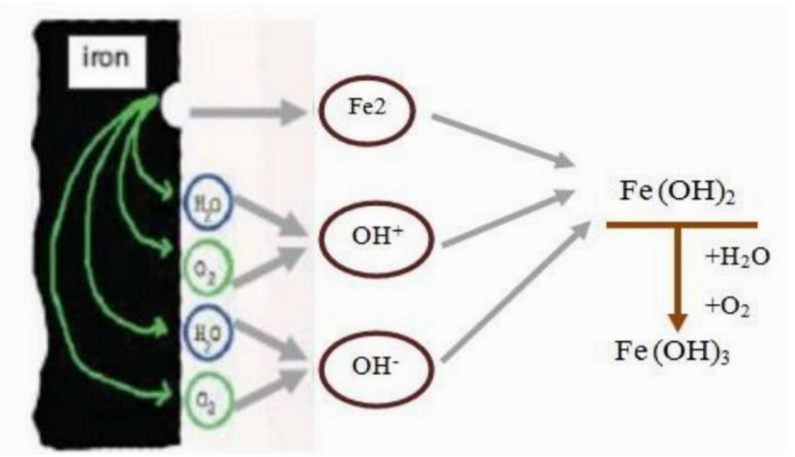

Figure 1. Corrosion mechanism in carbon steel

Slag from nickel smelting usually contains many of oxide (the example is NiO) that can react with Fe in ladle form FeO. Oxidation process to change Fe in ladle into FeO make the mass of ladle is decrease. If the process occurred in spot of ladle, it can inisiate pit in ladle or can be called pitting corrosion. Especially on this nickel matte smelter, there is one additional process to remove Fe contain in converter. Converter has two types of slag, low nickel slag and high nickel slag as mentioned before. Low nickel slag is more stable than high nickel slag because high content of fayalite (Albertsen 2008). Low nickel slag produced in early process of converter (Fe content still high), while high nickel slag produced in the middle process of converter (lower Fe content but higher Ni content). Despite extensive studies on slag chemistry in RKEF processes, this paper also collected operational data on nickel matte smelter regarding the role of converter slag deposits as a thermal-chemical protective barrier in ladle integrity. Figure 2 shows the geometric shape of the pouring vessel.

In 2023, a ladle leakage incident occurred during handling of high-nickel converter slag. For the information, ladles in operation right now are procured after 2020 (new ladle). This incident represents a significant safety concern and maked a delay in plant operations and the root cause has not yet been clearly identified by the company (systematic scientific investigation is required). This study aims to analyze the materials of both old and new ladles, evaluate the ladle failure mechanisms, and examine the formation of low-nickel converter slag deposits within the ladles.

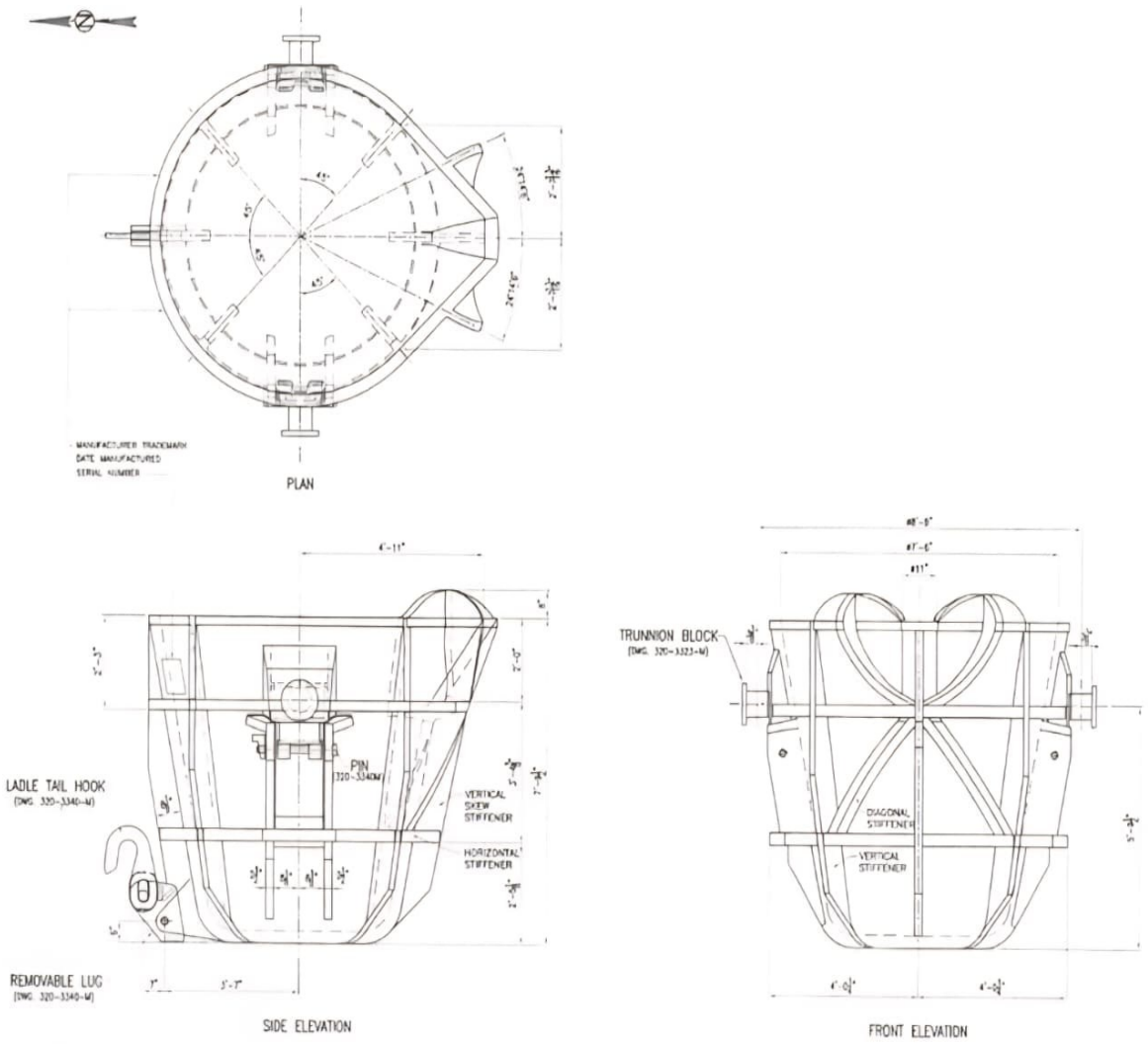

Figure 2. Ladle holder

METHODOLOGY

The materials used in this study consisted of trial ladles, low-nickel converter slag, and high-nickel converter slag. The equipment employed included a LiDAR camera (with accuracy until 1 mm), a thermal imaging camera (range temperature until 1500 ^{o}C), a crane, and oxy-acetylene cutting equipment. Material characterization was performed using an optical microscope, Scanning Electron Microscopy–Energy Dispersive X-ray (SEM–EDX), X-ray Diffraction (XRD), X-ray Fluorescence (XRF), and Optical Emission Spectroscopy (OES). Mechanical properties and ladle condition were evaluated through non-destructive testing (NDT), including wall thickness measurement, as well as tensile and hardness testing. All the equipments are well maintenance and calibrating to make sure the datas are valid and representative.

The material analysis of both old and new ladles involved microstructural observation using an optical microscope, chemical composition analysis using OES, and mechanical property evaluation through tensile and hardness tests.

Failure analysis of the ladles was conducted through microstructural examination using an optical microscope and surface morphology analysis using SEM–EDX. In addition, phase identification and chemical characterization of the slag were performed using XRD and XRF on low-nickel and high-nickel converter slag samples. The analysis of low-nickel converter slag deposit formation inside the ladle was carried out through a series of slag-holding trials up to the fifth cycle. During each holding cycle, the ladle wall temperature was measured using a thermal imaging camera, while deposit volume was determined using a LiDAR camera and calculated based on differences volume before and after measurement. To support this study, samples were collected from both old and new ladles from the nickel smelting industry. Figure 3 shows a sample from the old casting mold taken from the outer wall of the mold.

Figure 4 shows samples from a new casting mold and a damaged casting mold, taken from the same mold but from different locations. The sample from the new casting mold was taken from an undamaged section, while the sample from the damaged casting mold was taken directly from the area where the leak occurred.

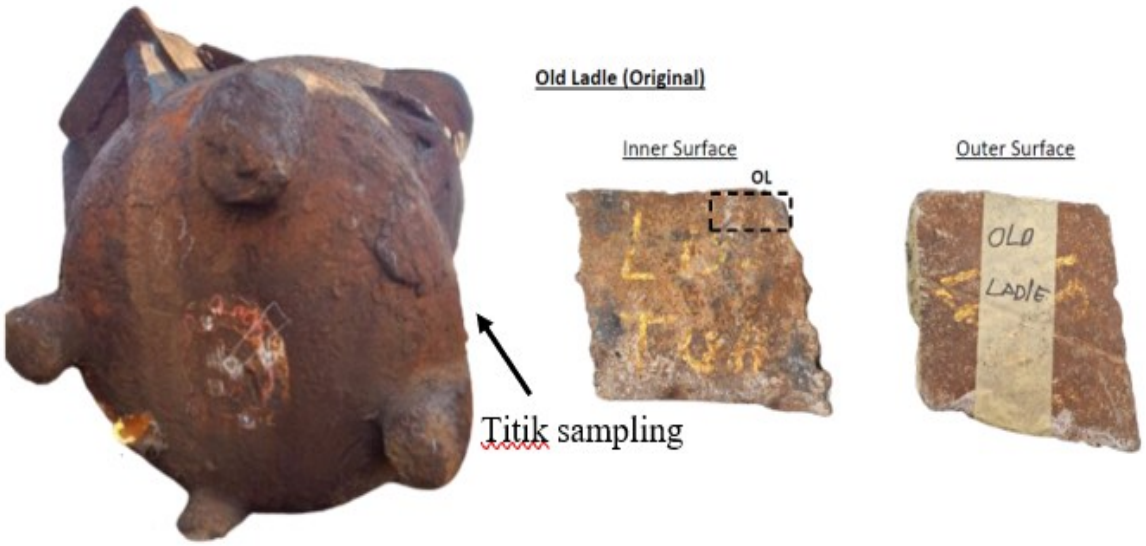

Figure 3. Old ladle sampling point

Figure 4. New ladle and leaking ladle sampling points

Table 1. Ladle research design

Parameters	Old ladle	New ladle	Leaky ladle
Ladle volume measurement without deposit		V	
Measurement of ladle volume and temperature after low nickel slag converter storage from 1–5		V	
Microstructure testing (metallography)	V	V	V
Visual observation	V	V	V
Optical emission spectrocopy	V	V	
Tensile Test and Hardness Test	V	V	
SEM – EDX			V
Thickness testing (non-destructive test)			V

Table 2. Research design of low and high nickel slag converter

Parameters	Low nickel slag converter	High nickel slag converter
XRD (X-Ray **d**ifraction)	V	V
XRF (X-Ray **f**luorescence)	V	V

The above test materials will be used in a research design as per Table 1.

XRD and XRF (Table 2) testing were conducted from the company internal laboratory, while other testing was conducted at the Department of Materials and Metallurgical Engineering, ITS.

RESULT AND DISCUSSION

Analysis of old and new ladle materials

The ladle material specifications that comply with the company recommendations refer to ASTM A27 Grade 60 – 30 which has standards (Tables 3 and 4).

Table 3. ASTM A27 grade 60 – 30 mechanical specification

Specification	Result
Tensile testing	min 415 Mpa
Hardness testing	120 – 150 HV

Table 4. Chemical composition of ASTM A27 grade 60–30

Element	%
C	Max. 0.30%
Mn	Max. 0.60%
Si	Max. 0.80%
P	Max. 0.05%
S	Max. 0.06%
Fe	Balance

Meanwhile, Table 5 is the result of chemical composition testing using optical emission spectroscopy on old and new ladle samples.

Table 5. Chemical composition test results of old and new ladles

Element	Old ladle (%)	New ladle (%)
C	0.28	0.18
Si	0.57	0.44
S	0.004	0.005
P	0.015	0.010
Mn	0.83	1.32
Cu	0.056	0.018
Cr	0.064	<0.0001
Al	0.102	0.085
Mo	0.022	0.002
Ni	0.042	0.019
Fe	Balance	Balance

Table 5 indicates that both the old and new ladles comply with the ASTM A27 Grade 60–30 standard specifications, as recommended by the company. With respect to manganese (Mn), which is known to enhance high-temperature resistance (Narasimha & Murigendrappa, 2021, the slightly higher Mn content does not adversely affect the quality or performance of the ladle material. But manganese (Mn) concentrating higher than 1% would accelerate corrosion rate of steel because it can be easier to build surface layers that highly contain of MnO and MnO_2. MnO and MnO_2 can serve as catalysts on the surface of steel corrosion layers, providing a more efficient pathway for electron transport (Guangbo, 2024). Meanwhile, a comparison between the old and new ladle reveals a significant difference in carbon content. The old ladle, containing 0.28% carbon, is classified as medium-carbon steel, whereas the new ladle, with 0.18% carbon, falls into the low-carbon steel category (Jin, 2020. No significant differences are observed in the concentrations of other alloying elements. Beyond chemical composition, the mechanical property aspects are discussed as follows.

Table 6. Tensile and hardness test results of old and new ladles

Hardness (HV)		Tensile strength (MPa)	
Old ladle	New ladle	Old ladle	New ladle
129	130	401	398

Table 6 indicates good agreement between the ASTM A27 Grade 60–30 standard (Table 3) and the hardness test result for both the old and new ladles. However, the measured tensile strengths for both ladle samples were slightly below the specified standard values. Tensile strength is slightly below the standard because of thermal cyclic due to operational uses. Thermal cyclic causes the material of ladle become fatigue. Material that fatigue has a high potential to get mechanical properties down grade like tensile streght (Pang, 2012). The microstructures of the old and new ladle were subsequently compared, yielding Figure 5.

Figure 5 presents the microstructures of both ladles. In both the old and new ladles, ferrite (light regions) and pearlite (dark regions) are observed. Quantitative analysis shows that the old ladle contains a lower ferrite fraction of approximately 60%, whereas the new ladle exhibits a higher ferrite content of about 75%, with the remaining fraction consisting of pearlite. Ferrite is a soft and ductile phase, while pearlite is comparatively

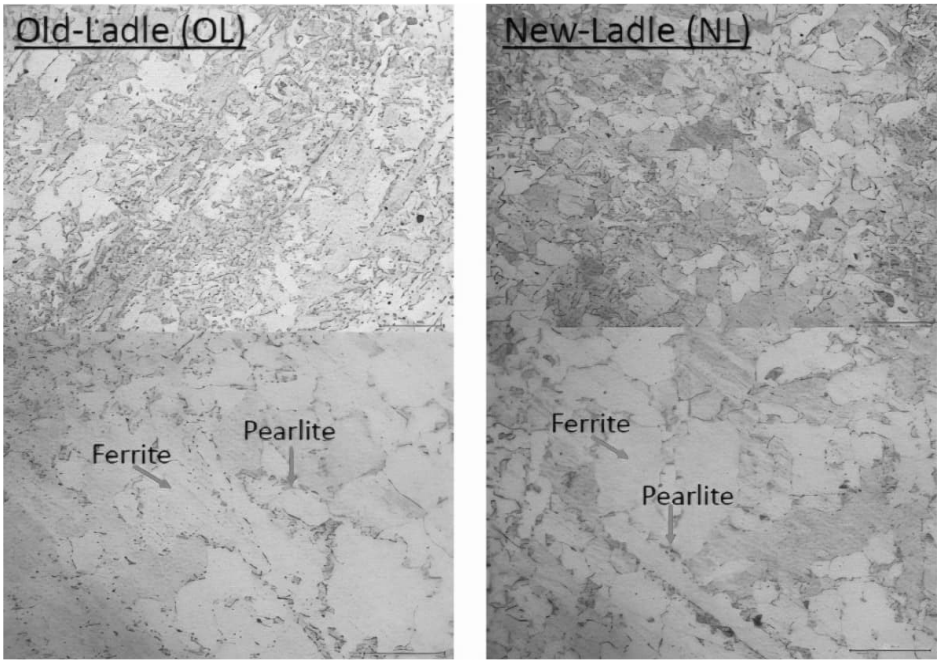

Figure 5. Microstructure of old and new ladle

harder (Steel et al., 2024. These observations are consistent with the chemical composition results in Table 5, as higher carbon content in steel reduces the ferrite fraction and promotes the formation of harder phases such as pearlite. Based on the data presented, both the old and new ladles comply with the company recommendations, which are based on the ASTM A27 Grade 60–30 standard. However, a difference in carbon content is observed between the two ladles, with the old ladle containing 0.28% carbon and the new ladle containing 0.18% carbon. This variation in carbon content is corroborated by microstructural analysis, where the old ladle comprises approximately 60% ferrite and 40% pearlite, while the new ladle consists of about 75% ferrite and 25% pearlite. Additionally, both ladles exhibit comparable mechanical properties, as summarized in Table 6.

Ladle leakage failure analysis

Immediately after the ladle leak incident, an investigation was conducted to document and analyze the ladle leak point (Figure 6).

As shown in Figure 2, the ladle is equipped with a hook at its tail that functions to tilt the ladle, allowing the molten liquid to be poured. At the time of the incident, failure occurred in the hook region.

Figure 7 indicates that the ladle thickness in the leaking area has been reduced to 39 mm from its original thickness of 90 mm. This region is particularly susceptible to high mechanical loads from slag and matte during the pouring process from the converter, as illustrated in Figure 8. In addition to the mechanical load concentrated in the ladle hook area during the initial slag pouring from the converter, it was observed that the low-nickel converter slag deposit within the ladle was relatively thin.

Visually, the deposits in the leaking ladle (Figure 9, left) differ significantly in thickness compared to those in normal ladles (Figure 9, right). This difference is further reflected in the ladle temperature at the time of the incident, which reached 565 °C, considerably higher than the average operating temperature of 335 °C (Figure 10).

The thin deposit of low-nickel converter slag allowed penetration by the high-nickel converter slag during pouring due to its higher temperature (approximately 1220 °C for high-nickel slag compared to 1200 °C for low-nickel slag). In the failure area, a pit was also observed that formed from the internal surface (Figure 11), indicating that the ladle failure originated from inside.

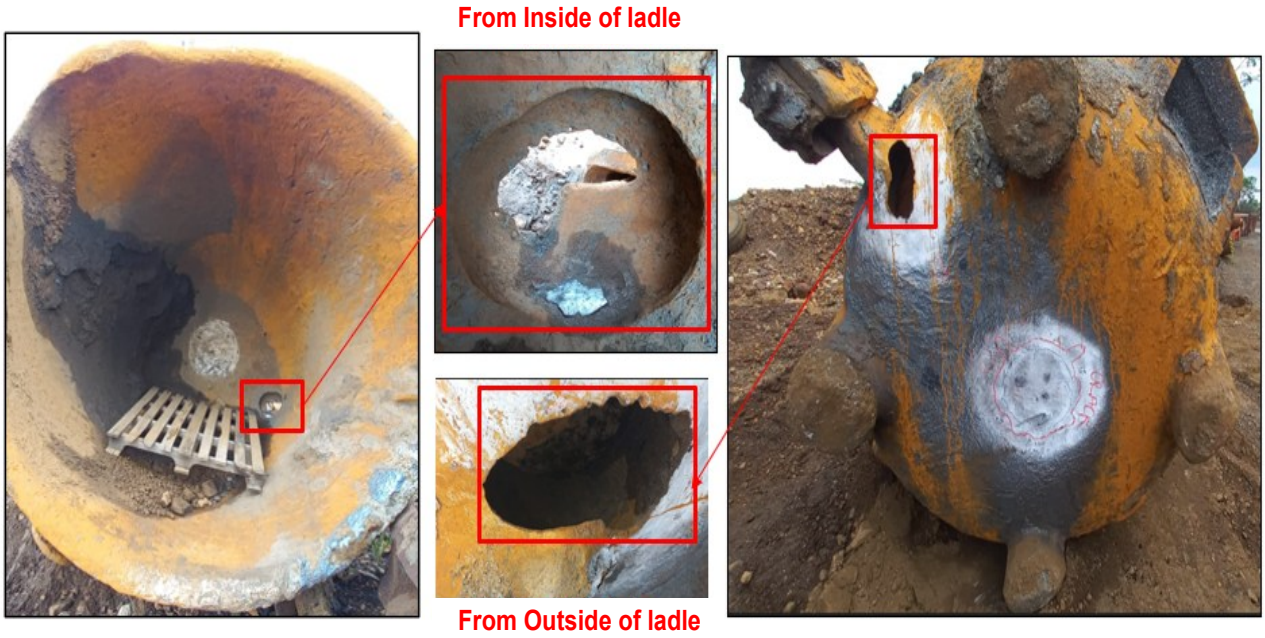

Figure 6. Visual observation of ladle leaking from inside and outside

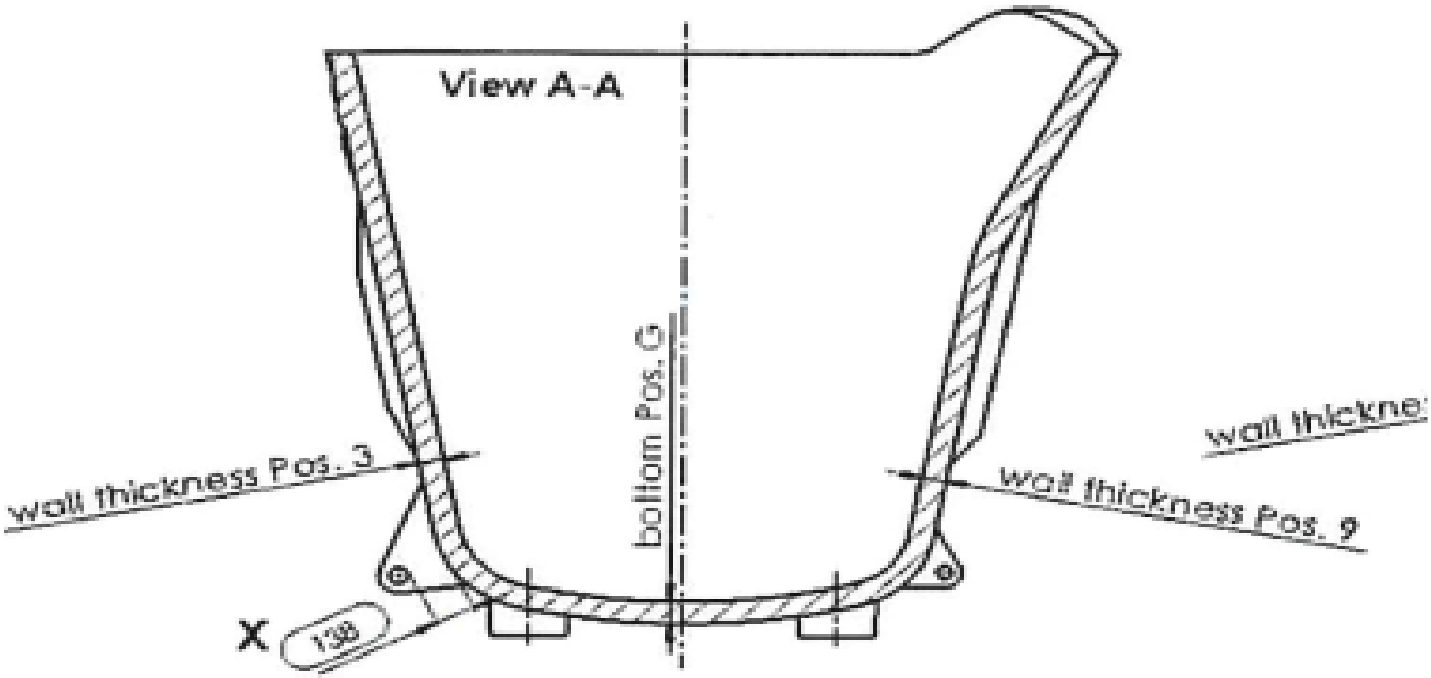

Leakage Position	NDT Thickness of ladle body (mm)			Remark
	Original Design	Pos. 3	Pos. 9	
3	90	39	NA	High Nickel Converter

Figure 7. Leakage point in ladle and its thickness

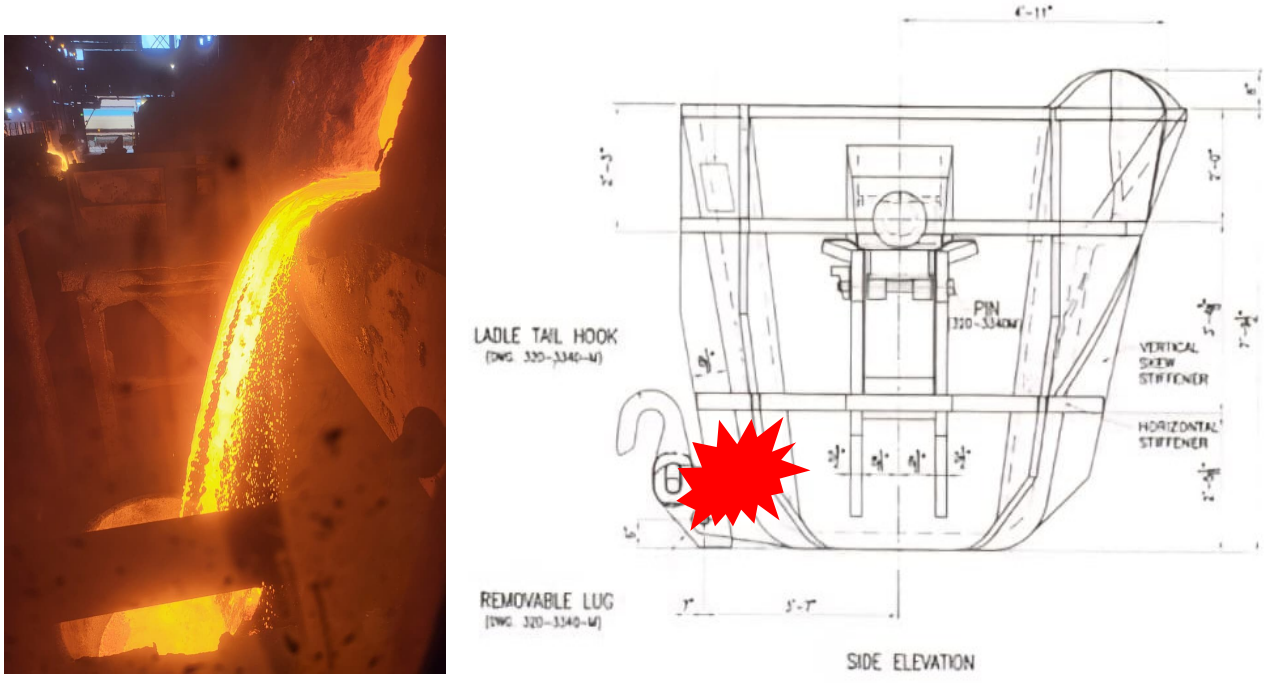

Figure 8. Slag pouring scheme from converter to ladle

Figure 9. Converter slag deposit on the wall of a leaking ladle (left) with another ladle (right)

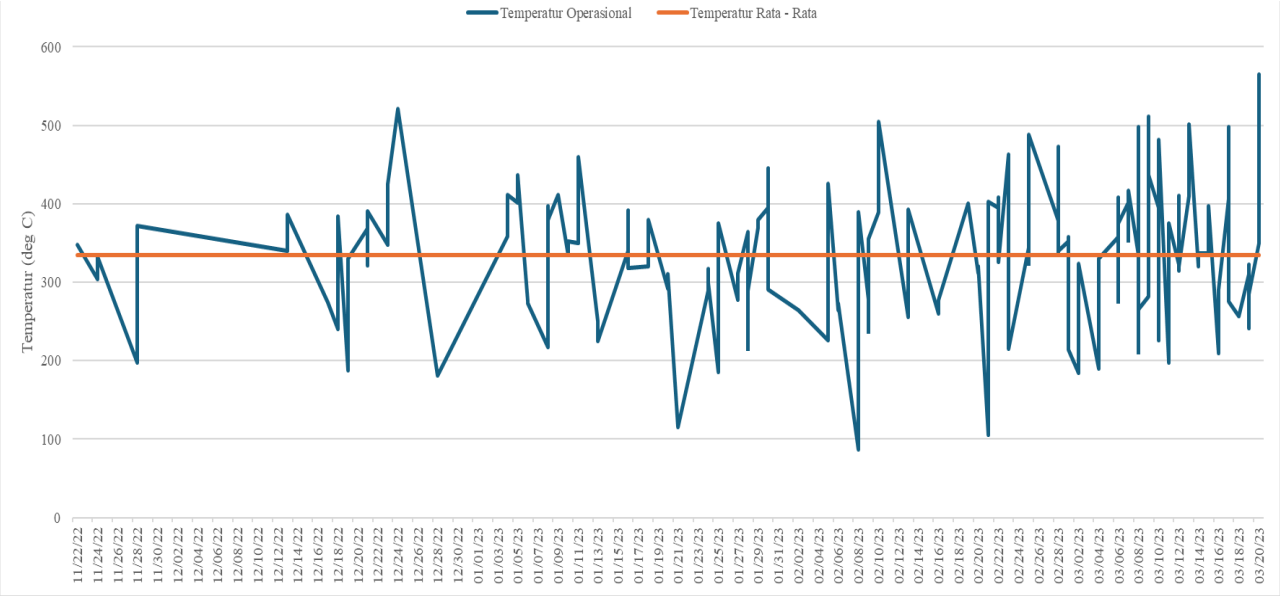

Figure 10. Ladle operating temperature

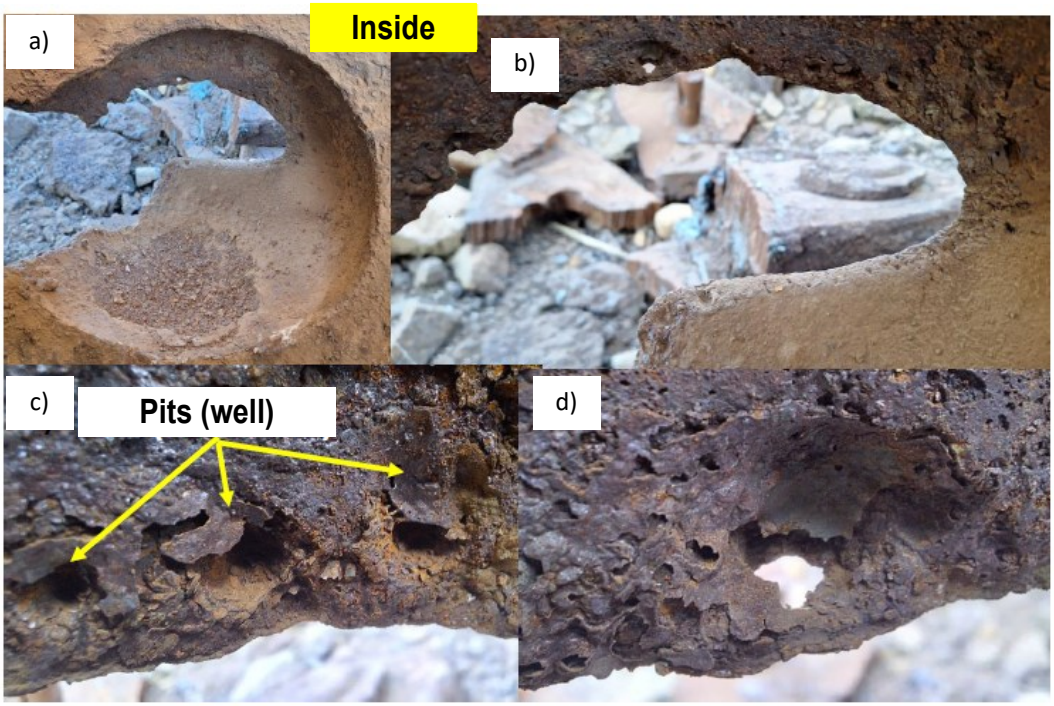

Figure 11. Visual observation of leakage points on ladle; (a) area of failure, (b) presence of multiple pits along the failure area, (c) more detailed visualization of pits, (d) sem – edx test points

The pits formed along the failure area (Figures 11c and 11d) are illustrated below. Some locations exhibit raised features, while others show deep pit formations. The points identified in Figure 11d will subsequently be selected for SEM–EDX analysis to characterize the surface morphology and elemental distribution in the affected region.

SEM–EDX results (Figures 13 and 14) indicate that the failure area is dominated by non-ferrous elements, primarily silica and magnesia. However, based on the ladle chemical composition shown in Table 5, silica and magnesia are not constituent elements of the ladle material. Consequently, XRF and XRD analyses were performed on both low-nickel slag and high-nickel slag to test the hypothesis that the silica and magnesia detected in the ladle failure area originated from converter slag.

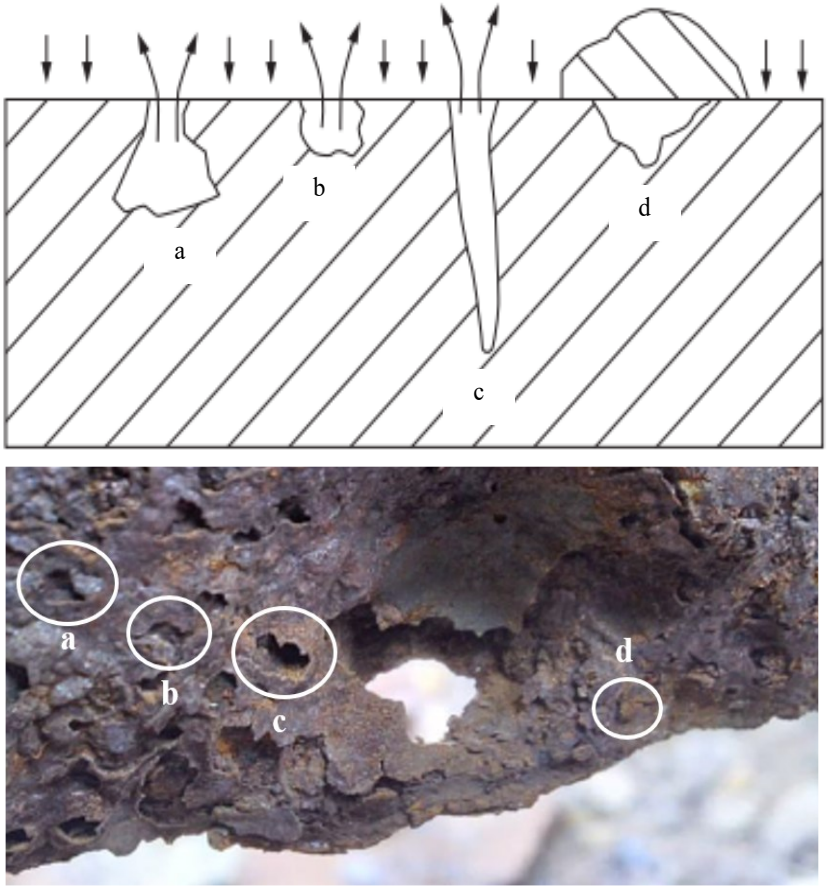

Figure 12. Mechanism of pitting corrosion (general aspects of corrosion, corrosion control, and prevention, part 1)

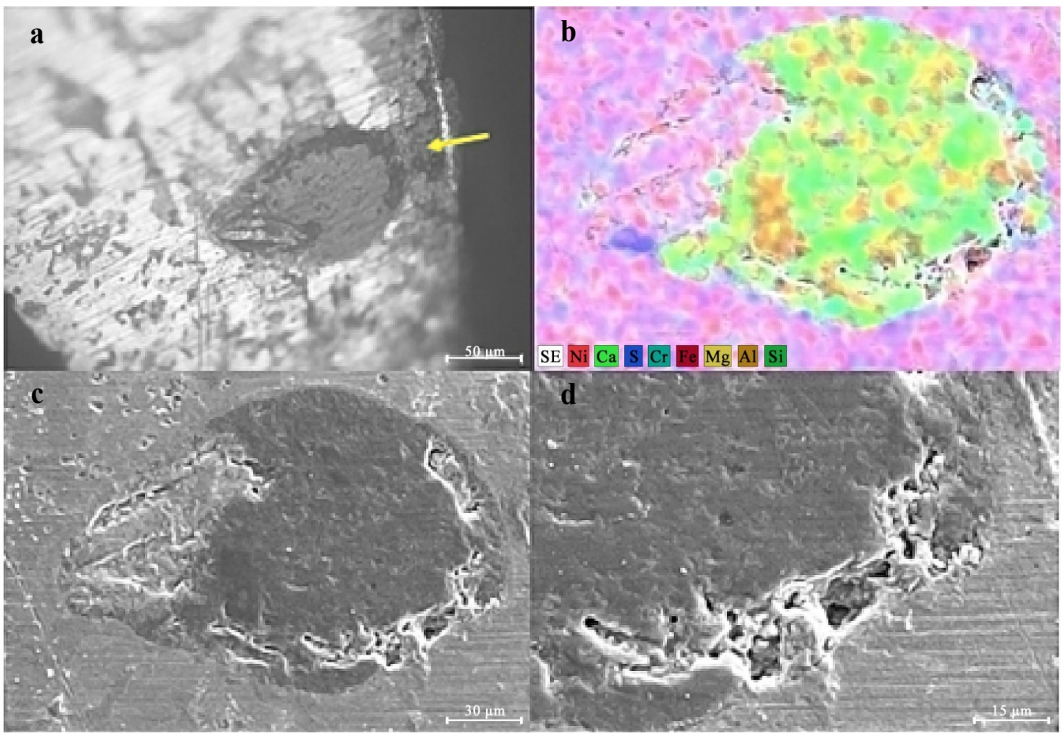

Figure 13. SEM – EDX test results in the Ladle failure area; (a). Test point with 75x magnification, (b). SEM – EDX results in the test area, ©. Test point with 100x magnification, (d). Test point with 150x magnification

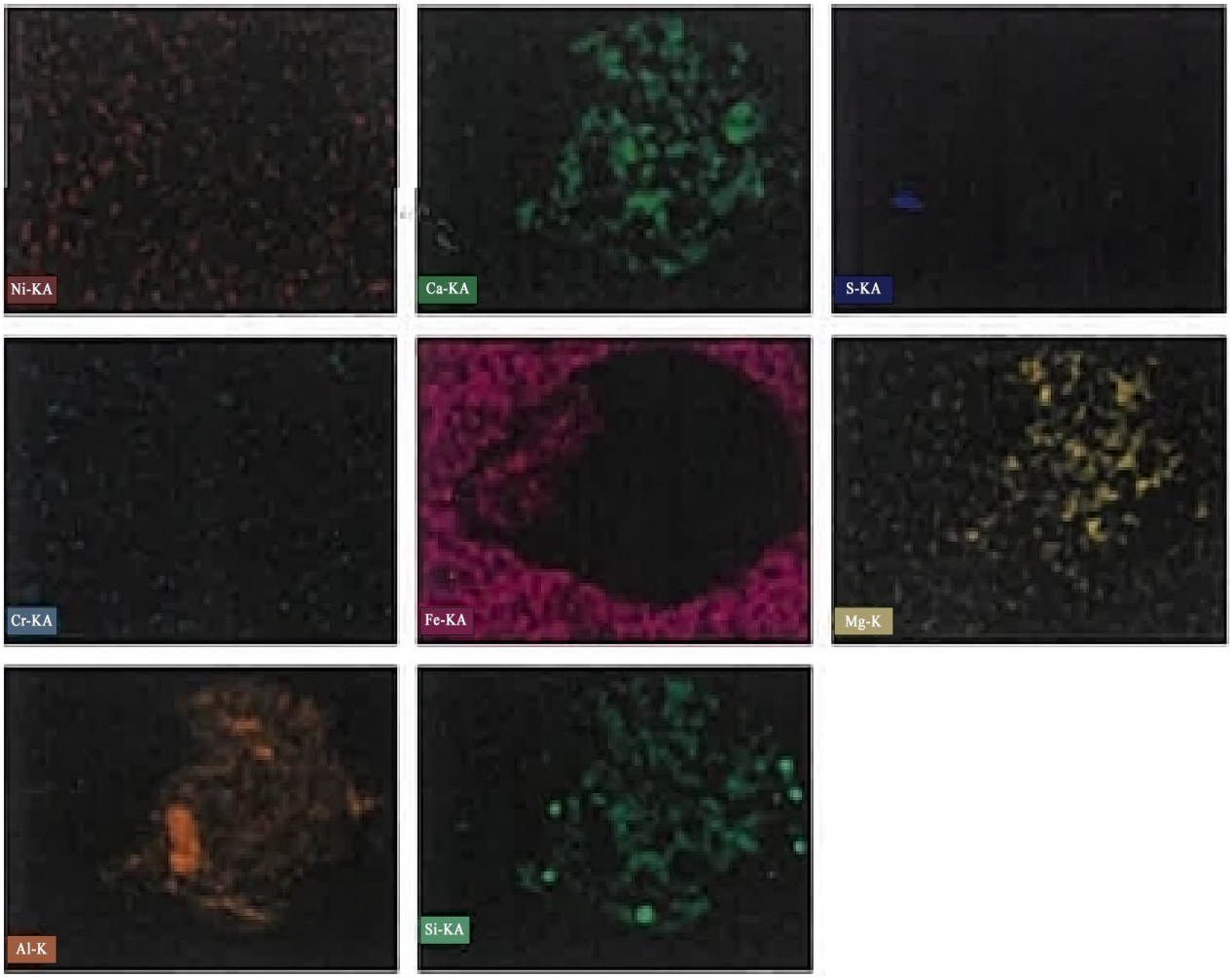

Figure 14. Distribution of elements in the failure zone

Table 7. Results of XRF low nickel slag converter

Element	%
Al_2O_3	0.31
Co	0.19
Fe	55.24
MgO	0.68
Ni	0.28
S	1.86
SiO_2	25.61

Table 8. Results of XRF high nickel slag converter

Element	%
Co	2.15
Fe	48.13
MgO	0.19
Ni	5.07
S	0.38
SiO_2	27.68

The XRF results above indicate that both low-nickel slag and high-nickel slag contain significant amounts of silica and magnesium, confirming that converter slag has penetrated into the ladle. In addition to the XRF findings, microstructural observations further reveal that notable microstructural changes have occurred, as illustrated in Figure 15 below.

A normal ladle exhibits a microstructure composed of ferrite and pearlite phases, as shown in Figure 4, whereas the failed ladle is dominated by a hard carbide phase. This phase transformation indicates that the failure area was exposed to elevated temperatures (Zheng et al., 2025. In addition to temperature effects, low-nickel slag and high-nickel slag differ significantly in chemical composition. As indicated by the XRD results in

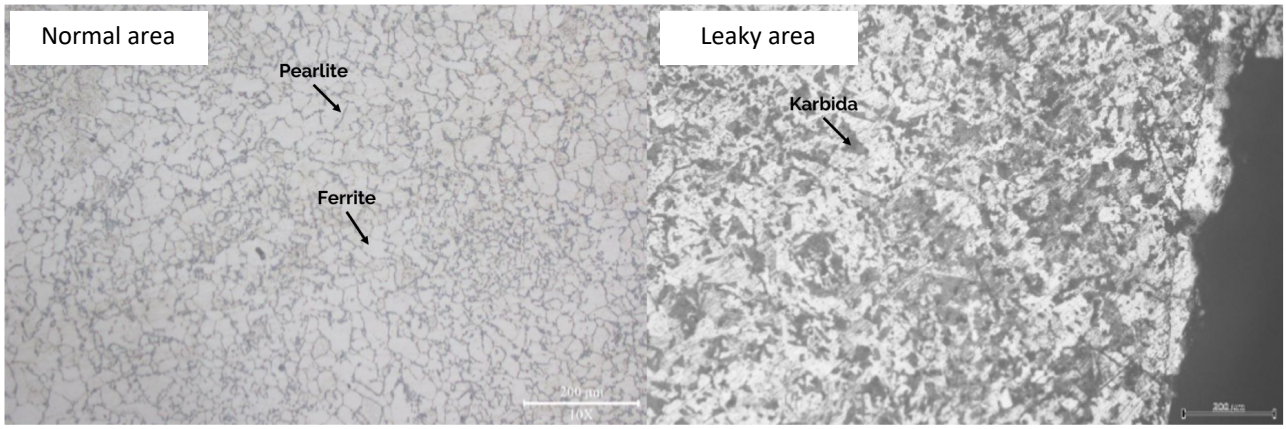

Figure 15. Microstructure between the normal ladle surface (left) and the failed ladle surface (right)

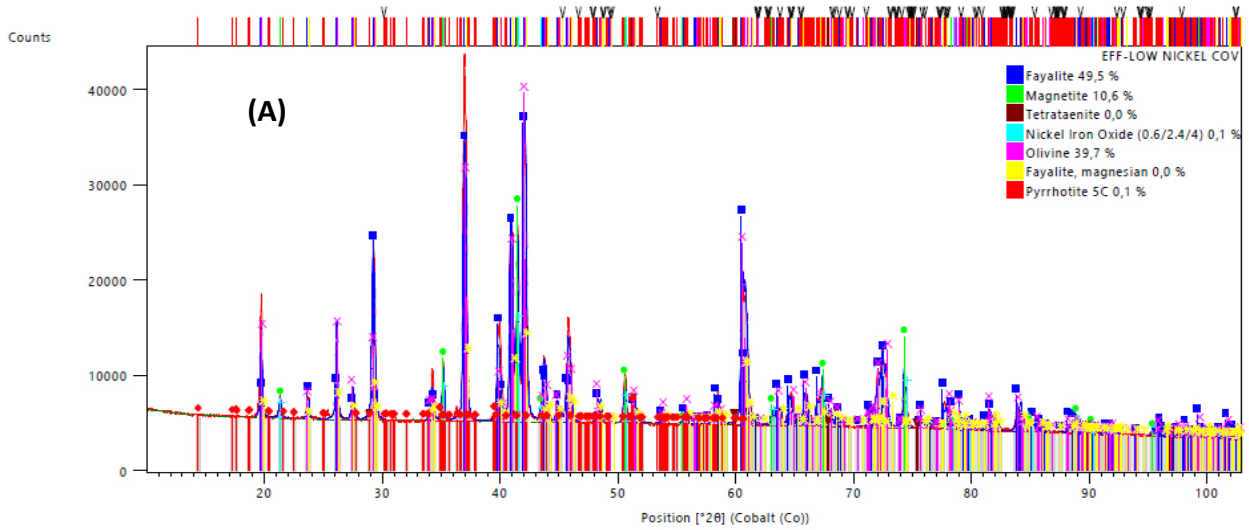

Figure 16A. XRD results of low nickel slag converter

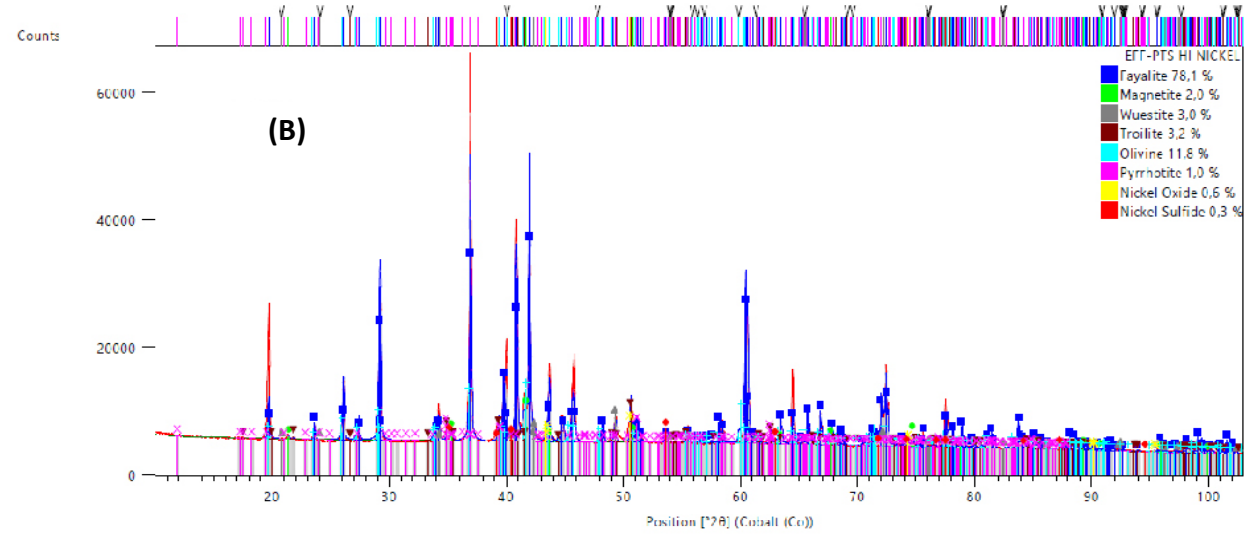

Figure 16B. Results of XRD high nickel slag converter

Figure 17, high-nickel slag contains a phase that is highly reactive toward iron (Fe) in the ladle, namely nickel oxide (NiO), which is not detected in low-nickel slag (Wang, 2017; Dalvi et al., 2004). Consequently, low-nickel slag poses a lower corrosion risk to iron–carbon ladles. Figure 16A presents the XRD pattern of the low slag converter.

Low nickel slag converters are mostly composed of fayalite (Fe_2SiO_4) and olivine ($(Fe.Mg)_2SiO_4$). Figure 15B is the XRD results from high nickel slag converters.

Figure 16 demonstrates that high-nickel converter slag differs in composition from low-nickel converter slag. Compounds such as nickel oxide and nickel sulfide are present only in the high-nickel converter slag. As discussed earlier, nickel oxide (NiO) is highly reactive with iron (Fe). Consequently, when high-nickel converter slag penetrates the original ladle material, which is predominantly composed of iron, the iron in the ladle undergoes oxidation according to the following reaction Equation 1.

$$Fe + NiO \rightarrow FeO + Ni \quad (1)$$

Greater oxidation of Fe to FeO leads to a progressive reduction in ladle mass and wall thickness in the affected area. This interpretation is supported by SEM–EDX results, which show a significant decrease in iron (Fe) content at the failure location, accompanied by a uniform distribution of nickel (Ni). The oxidation of Fe to FeO is further evidenced by the formation of pits along the failure zone (Figures 11 and 12). With continued contact between the high-nickel converter slag and the ladle wall, these pits develop extensively; smaller pits coalesce to form larger perforations, as illustrated in Figure 11a. In contrast, reaction (1) does not occur when a sufficiently thick low-nickel converter slag deposit layer is present on the ladle wall (Figure 18).

Analysis of low nickel slag converter deposit formation in ladle

As discussed in the previous failure analysis, insufficient thickness of low-nickel converter slag deposits in the ladle was identified as one of the contributing factors to failure. Currently, the company has not established a specific standard for deposit thickness or volume. Therefore, the initial step involved measuring the volume of an empty ladle without low-nickel converter slag deposits, as presented below.

Table 9. Ladle temperature measurement data from the first to the fifth reservoir

Ladle	High temperature	Average temperature
Blank	nd	nd
First	452 °C	365.76 °C
Second	430 °C	356.45 °C
Third	380 °C	321.50 °C
Forth	372 °C	299.10 °C
Fifth	328 °C	269.95 °C

The measured volume corresponds to the space extending from the base of the ladle to the trunnion, as illustrated in Figure 19. The results indicate that the empty (blank) ladle has a volume of 4.31 m³. Subsequent volume measurements were conducted during the first through fifth low-nickel converter slag holding cycles, yielding the results presented (Figure 19).

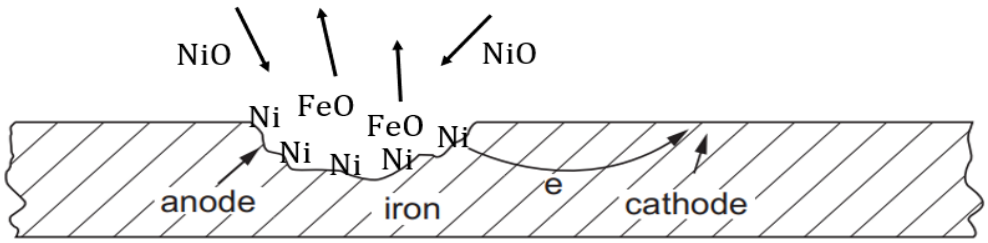

Figure 17. Illustration of failure in ladle

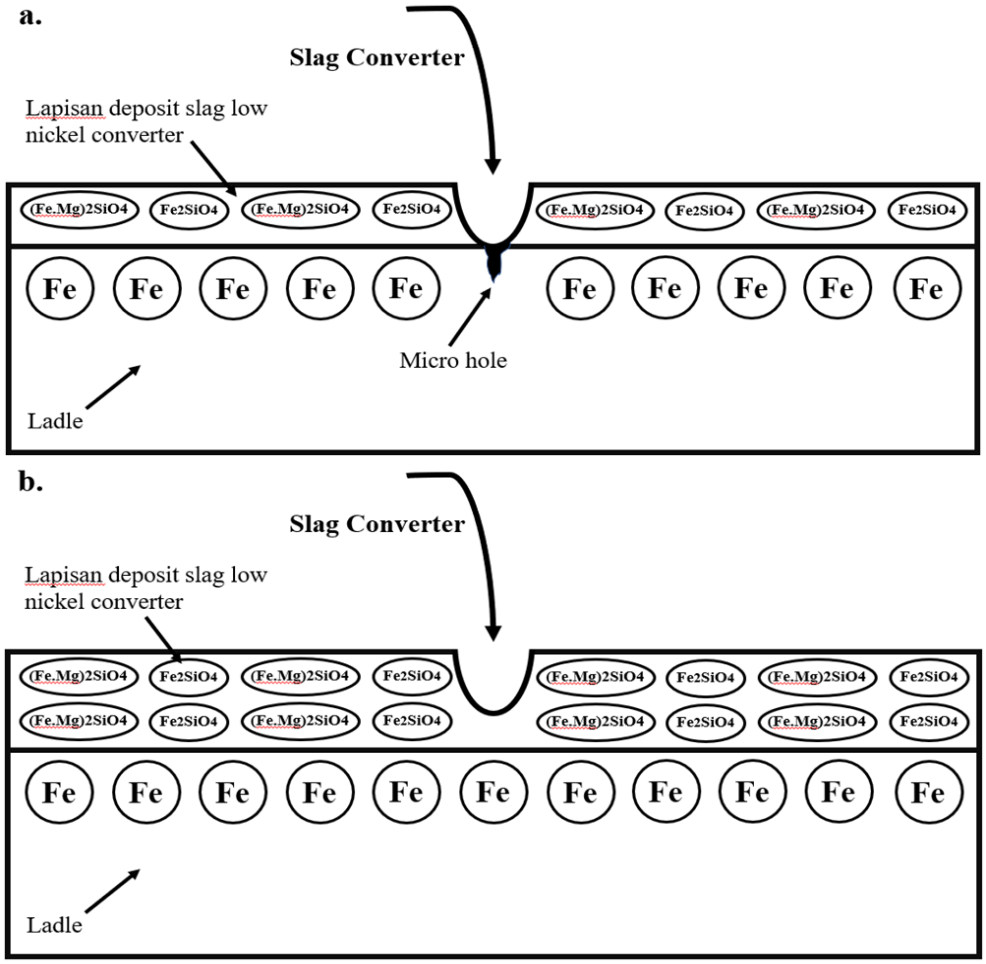

Figure 18. Illustration of the Effect of Thin low nickel slag converter deposits (a) and thick low nickel slag converter deposits (b)

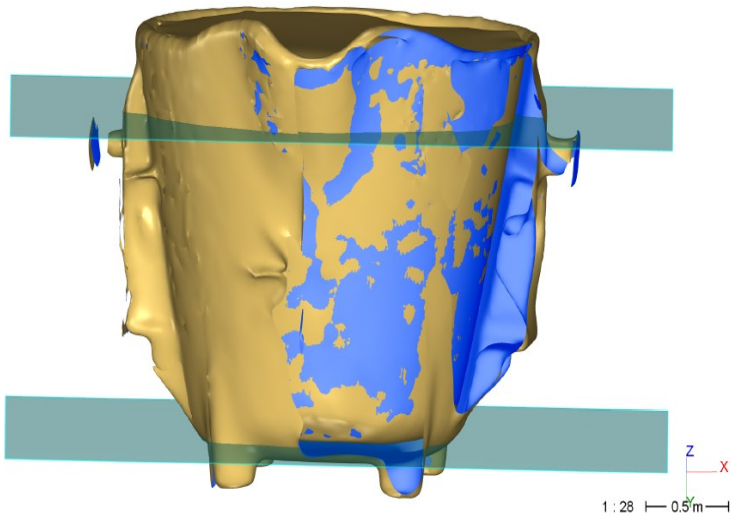

Elevation (m)	Volume over (m^3)	Volume under (m^3)
0.000	5.978	0.000
1.700	1.667	4.310

Figure 19. Measurement results for the blank ladle volume

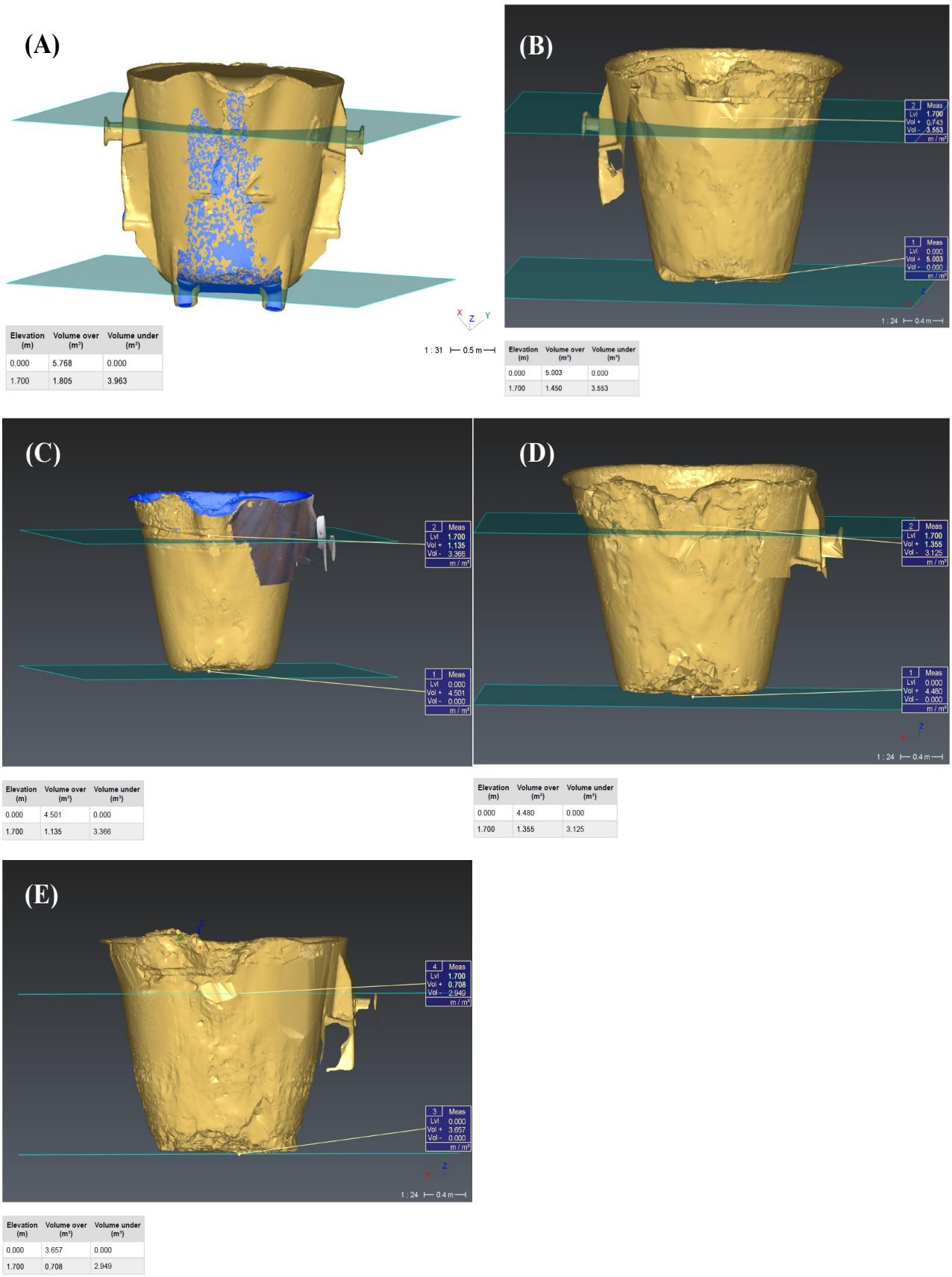

Elevation (m)	Volume over (m³)	Volume under (m³)
0.000	5.768	0.000
1.700	1.805	3.963

Elevation (m)	Volume over (m³)	Volume under (m³)
0.000	5.003	0.000
1.700	1.450	3.553

Elevation (m)	Volume over (m³)	Volume under (m³)
0.000	4.501	0.000
1.700	1.135	3.366

Elevation (m)	Volume over (m³)	Volume under (m³)
0.000	4.480	0.000
1.700	1.355	3.125

Elevation (m)	Volume over (m³)	Volume under (m³)
0.000	3.657	0.000
1.700	0.708	2.949

Figure 20. Ladle volume after accommodating low nickel slag converter; (a). First; (b). Second; (c). Third; (d). Fourth; (e) fifth

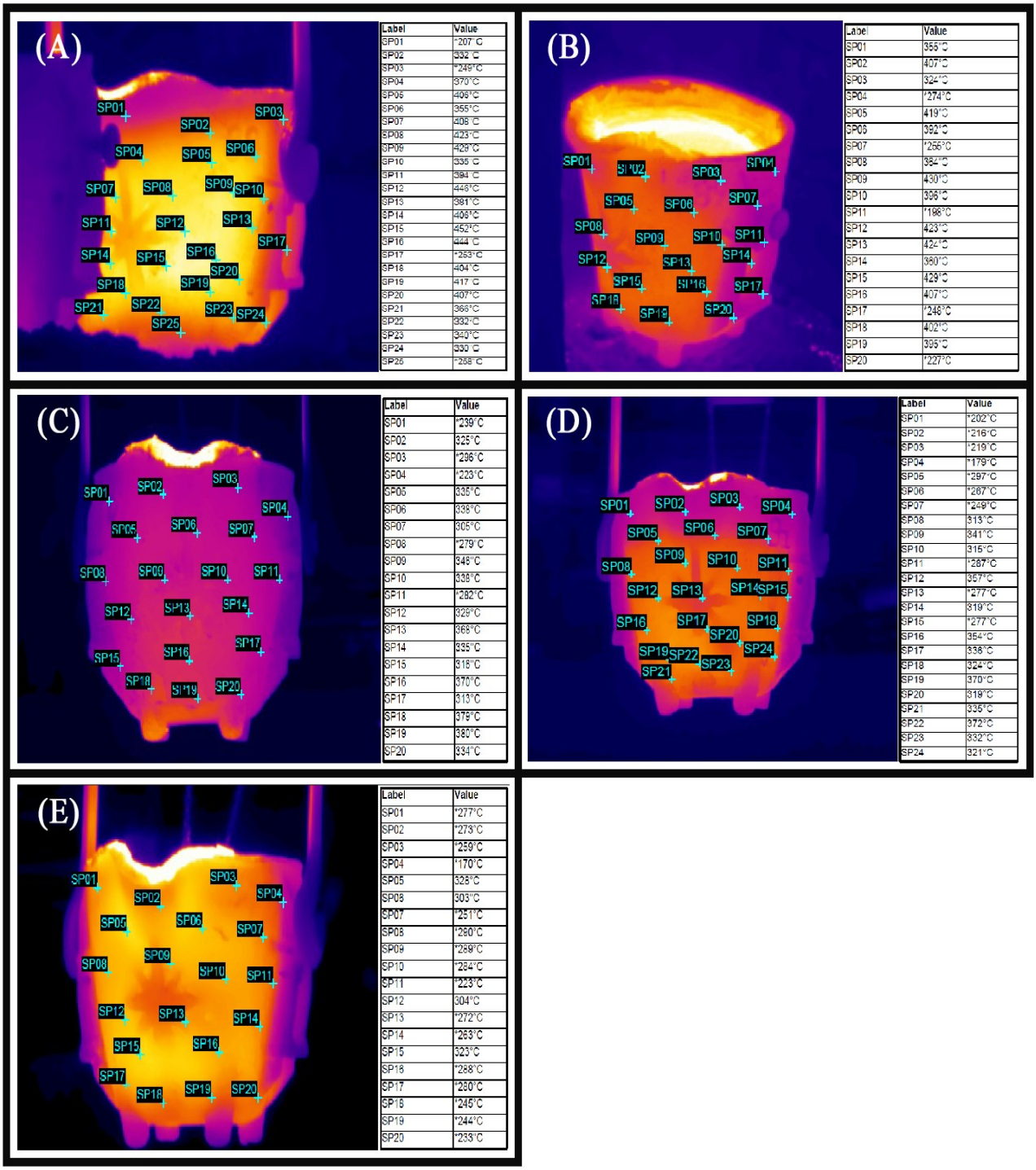

Figure 21. Ladle temperature measurement; (a) first reservoir; (b) second reservoir; (c) third reservoir; (d) fourth reservoir; (e) fifth reservoir

Table 8 shows that the volume of low-nickel converter slag deposits increases with increasing collection frequency. Excessive deposit thickness can lead to operational issues by reducing the effective capacity for slag or matte and limiting the number of ladles available for operation. Conversely, deposits that are too thin may fail to provide adequate protection and can promote ladle leakage, as discussed in this study. The temperature data measured at each collection stage are presented below.

The data in Table 9 indicate that ladle temperature decreases with increasing collection frequency. When correlated with the results in Table 8, this trend demonstrates that a higher volume of low-nickel converter slag deposits contributes to a reduction in overall ladle temperature. Operational data (Figure 10) show that ladles at the company operate at an average maximum wall temperature of approximately 335 ° C. Accordingly, the temperature measurements indicate that ladles can safely handle high-nickel converter slag and matte with a low risk of leakage when low-nickel slag collection has reached the fifth cycle. Meanwhile, Figure 21 is a capture from a thermal imaging camera related to measuring the ladle temperature.

CONCLUSION

The main conclusions of this study are summarized as follows. First, both old and new ladles comply with the company specifications based on ASTM A27 Grade 30–60 (minor attention with manganese (Mn) contain in both ladle that slightly higher than standard). Nevertheless, the old ladle is classified as medium-carbon steel (0.28 wt.% C) and the new ladle as low-carbon steel (0.18 wt.% C). This carbon percentage also figuring with their microstructures, higher pearlite content in the old ladle (strong evidence to higher carbon percentage) and higher ferrite (phase in low carbon percentage) content in the new ladle. Second, ladle failure was primarily caused by localized mechanical load at the hook area during initial high-nickel slag pouring, combined with the absence of a protective low-nickel slag deposit layer. This condition allowed high-nickel slag penetrated and promoted chemical interaction between nickel oxide (NiO) and iron (Fe), forming iron oxide (FeO) and inducing pitting corrosion that led to leakage. Third, increasing the frequency of low-nickel slag handling increased deposit volume and reduced ladle wall temperature. After the fifth low-nickel slag cycle, the ladle operated at a safe temperature (~335 °C) with a reduced risk of leakage during high-nickel slag and matte handling.

ACKNOWLEDGEMENT

The authors gratefully acknowledge the management of the company that give the supportive to this paper, and the Department of Materials and Metallurgical Engineering, Institut Teknologi Sepuluh Nopember (ITS), for their support.

GLOSSARY OF TERMS AND SYMBOLS

Terms & Symbols	Definition	Unit
ASTM	American standard testing and material	
XRF	X-Ray fluorescence	
XRD	X-Ray difraction	
OES	Optical emission spectrocopy	
SEM	Scanning microscope electron	
EDX	Energy dispersive x-ray	
LiDAR	Light Detection and Ranging	
NDT	Non – destructive test	
RKEF	Rotary kiln electric furnace	

REFERENCES

Pujilaksono Bagas, (2016), The Degradation of The Propective Scale on Binary FeCr Alloys (Fe-2.25Cr, Fe-10Cr, Fe-18Cr and Fe-25Cr) in CO_2 and in $CO_2 + H_2O$ Environment at 600^oC. Journal of Scientific Contributions Oil and Gas. Vol. 39, Number 1 : 2 of 5. https://

doi.org/10.29017/SCOG.39.1.530.

Dalvi, A. D., Bacon, W. G., Osborne, R. C., Limited, I., Boulevard, F., & Park, S., (2004), The Past and the Future of Nickel Laterites World ' s Land Based Nickel Resources and Primary Nickel Production Nickel Production , kt / yr. Figure 2, 1–27.

Guangbo, Zhang., Huanhuan, Zhang., Xingyu, Liu., (2024), Effect of Mn on Corrosion Resistance of Low - Cr Weathering Steel. https://doi.org/10.3390/met14121433.

Iman, Y., & Huda, I., (2019), ScienceDirect Preliminary Study of Smelting of Indonesian Nickel Laterite Ore using an Electric Arc Furnace. Materials Today: Proceedings, 13, 127 –131. https://doi.org/10.1016/ j.matpr.2019.03.201.

Industry, C., Shchelokova, E. A., Timoshchik, O. A., & Semushin, V. V., (2023), Deep Processing of Dump Slag from the Copper-Nickel Industry.

Huwen, Ma. Yanchun, Zhao, (2024), Effect of Mn Content on Corrosion and Mechanical Behaviors of Fe - based Medium Entrophy Alloy. Journal of Materials Research and Technology 30 (2024) 5632 - 5651.

Jin, A., (2020), The Discussion On The Influence Of The Form And Content Of Carbon On The Properties Of Carbon Steel And Cast Iron The Discussion On The Influence Of The Form And Content Of Carbon On The Properties Of Carbon Steel And Cast Iron. 0–4. https:// doi.org/10.1088/1755-1315/580/1/012058.

Laterite, N., Processes, S., & Route, C., (2019), Nickel Laterite Smelting Processes and Some.

Narasimha, B., & Murigendrappa, S. M. (2021). Effect of manganese and homogenization on the phase stability and properties of Cu e Al e Be shape memory alloys. Journal of Materials Research and Technology, 14, 1551–1558. https://doi.org/10.1016/j.jmrt.2021.07.027.

Noegroho, Hadi, (1983), Faktor Utama Penyebab Korosi Atmosfer di Kawasan Industri. Lembaran Publikasi Lemigas No. 2/XVII/ Agustus 1983. https://doi.org/10.29017/ LPMGB.17.2.1524.

Nofrizal Nofrizal, Susan A Impey & Konstantinos Georgarakis, (2019), The Prefential Weld Corrosion of X65 Carbon Steel Pipeline Under CO_2 Environment. Journal of Scientific Contributions Oil and Gas. Vol. 42, Number 1 : 3-5. https://doi.org/10.29017/SCOG.42.1.387

Of, D., Industry, (2024), Jurnal Legalitas Added Value In Indonesia. 17(1), 1–16. https:// doi.org/10.33756/jelta.v16i1.xxxx.

Pambudi, P. A., (2025), The Paradox of Nickel Investment in Indonesia. 5(November), 299–319.

Pang, J, C,. Wang. Zhang, (2012), General Relation Between Tensile Strength and Fatique Strength of Metallic Materials. Material Science and Engineering A 564 (2013) 331 - 341.

Ratna, Kartikasari, (2009), Studi Pengaruh Temperatur Temper Terhadap Sifat Mekanik dan Ketahanan Korosi Paduan Fe-1,26AI-1,05C. Jurnal Teknik Mesin.

Series, I. O. P. C., & Science, M., (2018), Nickel extraction from nickel matte. https:// doi.org/10.1088/1757-899X/285/1/012001.

Steel, H., Experiments, U., Field, P., Qayyum, F., Darabi, A. C., Guk, S., Guski, V., Schmauder, S., & Prahl, U., (2024), Analyzing the Effects of Cr and Mo on the Pearlite Formation in Numerical Simulations.

T, A. R. Z., Malina, J., & T, T. S., (2013), Characterization of Ladle Furnace Slag from Carbon Steel Production as a Potential Adsorbent. 2013.

Wang, Z., (2017), Preparing Ferro-Nickel Alloy from Low-Grade Laterite Nickel Ore Based on Metallized Reduction – Magnetic Separation. https://doi.org/10.3390/met7080313.

Zheng, Y., Chu, S., Zhang, L., Wang, Q., Qiu, G., Zhu, L., Guo, Z., Xie, T., Zhao, H., Lu, S., & Wang, B., (2025), Research on microstructure evolution and carbide transformation behavior during the quenching and tempering processes of secondary hardening steel. Journal of Materials Research and Technology, 36(May), 8088–8107. https://doi.org/10.1016/j.jmrt.2025.05.059.